Two realistic scenarios of intentional release of radionuclides (Cs-137, Sr-90) – the use of the HotSpot code to forecast contamination extent

D. DI GIOVANNI[1,4], E.LUTTAZZI[4], F.MARCHI[4], G. LATINI[3,4], M. CARESTIA[1,4], A. MALIZIA[1,4], M. GELFUSA[1,4], R. FIORITO[2,4], F. D'AMICO[1,4], O.CENCIARELLI[1,4], A. GUCCIARDINO[1,4], C. BELLECCI[1,4] and P. GAUDIO[1,4]

1. Associazione EURATOM_ENEA, Department of Industrial Engineering, University of Rome "Tor Vergata", Via del Politecnico 1, 00133, Roma, ITALY.
2. Department of Bio-Medical & Prevention, School of Medicine and Surgery, University of Rome "Tor Vergata", Via di Montpellier 1, 00133, Roma, ITALY.
3. AERO SEKUR Spa, Prototype & Manufacturing Unit, Via delle Valli, 46 - 04011 Aprilia (LT).
4. International Master courses in "Protection against CBRNe events", Department of Industrial Engineering, University of Rome "Tor Vergata", Via del Politecnico 1, 00133, Roma, ITALY.

Corresponding authors : daniele.digiovanni@students.uniroma2.eu;

Abstract: There are several types of events that could result in dispersion of radioactive substances in the environment. The dispersion can be a consequence of a natural or intentional event. In case of radiological release the estimation of the contaminated area is very important to properly manage the rescue operations and decontamination by evaluating the impact on the population and environment.
The extent of the contamination and impact on the environment and people mainly depends on the specific event and the radionuclide involved. Models and computational codes have been developed and hypothetical scenarios have been formulated for establishing priority of countermeasures and protective actions, determining generic operational guidelines and assessment of risks for population exposure.
The aim of the present study is to illustrate the effects of two different cases of intentional release. Due to the lack of available real data, this is carried out through simulation of different scenarios by using a computer code named HotSpot; in fact literature data referring to real events of this kind are classified and cannot be disseminated. The first case consists in the release of Cs-137 from stacks of cement production industry, the second in the release of Strontium 90 from the explosion of a dirty bomb. The Total Effective Dose Equivalent (TEDE), which includes external and internal contributions for the whole absorbed dose, and the contaminant Ground Deposition have been calculated for various atmospheric stability Pasquill categories [1], several distributions of contaminant particle size, different explosive quantity (dirty bomb case). Results have been analyzed and presented here. They indicate that atmospheric dispersion of a relatively small amount of Cs-137 has the potential to contaminate a relatively large area, while the explosion of a dirty bomb containing a large amount of a strontium 90, does not represent a problem in terms of direct contamination. In both cases the extent of contamination (area and activity) mainly depends on: particle size; the height of release and local weather conditions.

Keywords: Dispersion Models, Radionuclides, Atmospheric Release, Cesium 137, Strontium 90, HotSpot code

1. Introduction

Incidents involving commercial radioactive sources that have fallen out of control (orphan sources [41]) and entered into the public domain have been reported over the years. In some cases, sources entering into scrap processing facilities have contaminated steel mills, resulting in millions of dollars in cleanup costs. In other cases, sources have been breached, exposing the public to harmful radiation. These experiences are also interesting in relation to 'dirty bomb' scenarios, as these accidents led to the contamination of a city area of a size equivalent to what might be affected by the contamination from a successful 'dirty bomb' attack.

The U.S. government and the International Atomic Energy Agency (IAEA) had shown their interest in a more strict management system for commercial radioisotope materials. Significant amounts of non-fissile radioactive materials are stored in medical centers to diagnose and treat illnesses, research laboratories, processing plants to irradiate food to eliminate microbes, radiothermal generators, and oil well surveying instruments. Although those facilities lack the types or volumes of materials suitable for producing nuclear weapons, they contain large amounts of radioactive material such as cesium-137, cobalt-60, strontium-90, and iridium-192. A radiological attack would not produce the mass casualties due to the blast and significant radiation exposure associated with a nuclear event, but it nonetheless could result in radiation concentrations exceeding International Commission on Radiological Protection (ICRP) guidelines for limiting exposures to gamma radiation. The toxicity of a given radioactive material and the associated doses for internal organs depend on some factors as: 1) type and energy of the radiation emitted by radionuclides, 2) the route of entry into the body, and 3) the chemical characteristics of the element, that determines the retention and distribution in the body. Such an incident could create a variety of impacts ranging from extensive contamination requiring remediation, to panic and economic disruption, to long-term exposure of civilian populations to low levels of radiation exceeding natural background levels. The actual impact of terrorists releasing non-weapons grade materials is contingent upon a variety of factors including: the specific isotope used; the amount of material released; the aerosol properties of the particles released; local-scale meteorological conditions within a distance $\leq$10 km from the initial release point (i.e., wind speed, wind direction, other key meteorological parameters); local-scale typography (i.e. location and size of buildings); and the type of device used to release the material (i.e., conventional explosive).

These are the main reasons connected to the evolution of the techniques and methods for the atmospheric dispersion modeling. The three marked types of dispersion models, are: Gaussian plume models in the 1960s and 1970s, Lagrangian – puff models and particle random walk models in the 1980s - 1990s, and CFD (Computational Fluid Dynamics) models in the 2000s [3, 5-19].

In this study, potential scenarios of radiological release are simulated using HotSpot, which is able to estimate the radiation dispersion in an area. The main purpose of this work is evaluate the efficiency of HotSpot code using different dispersion models applied to different accidental scenario's.

Concerning contaminants that might be released to the atmosphere in case of a radiological event, a very large number of different radionuclides could be involved. It is unlikely that terrorists can gain access to huge amounts of radioactive materials, thus the sources would in general be small, and might possibly be stolen from an authorized user or manufacturer, or bought on the black market. This study will consider the effects of intentional dispersion of two kind of strong radioactive sources, considering their availability all over the world:

- Cs - 137 source (in readily soluble powder form);
- Sr - 90 source (in a ceramic matrix).

The main characteristics of Cesium and Strontium are reported in [40].

About Cesium-137 and its availability, it's possible to refer to the "Goiânia case" in Brazil [2]. Here a 50.9 TBq 137CsCl 'orphaned' source (in readily soluble powder form) suddenly appeared completely out of context in an inhabited area, causing contamination of a considerable area and many people, of which four were reported to have died within a week. The Goiânia accident resulted in extensive panic, social disruption, great efforts and expenses for personal monitoring, decontamination of humans and area clean-up, for instance of roof tiles with Cs-137 contamination levels ranging up to some 700 kBq m-2. In the wake of the terrorist attack on September 11th, 2001, there is a further security concern over radioactive materials. Traditionally, most commercial radioactive materials are not considered as potential sources of nuclear weapons, and thus are managed less stringently than uranium or plutonium. However, terroristic events raised the concern that such commercial radioactive materials could be cause of social disorder, being used in terrorist weapons, such as dirty bombs.

In relation to the Strontium-90, it's possible to mention that in the former Soviet Union it is approximately estimated the presence of 1,000 Radioisotope Thermoelectric Generators (RTGs), most of which are used as power sources for lighthouses and navigation beacons. The nucleus of an RTG is a source of thermal energy that uses the radioactivity of strontium 90, known also as RHS-90 (Radioisotope Heat Source-90). RHS-90s are sealed radiation sources in which the composition of the fuel may have two forms: strontium titanate ceramic -90 (SrTiO3), and strontium borosilicate glass. The sources are protected against external impact by the thick shell of the RTG , manufactured

in stainless steel, aluminum and lead . The shield of biological protection is configured in such a way that the radiation levels do not exceed 2 mSv/h on the devices , and 0.1 mSv/h at a distance of one meter. All Russian RTGs have long exhausted their 10-year engineered life spans and are in dire need of dismantlement, both to avoid accidents and to prevent the theft of radioactive material abandoned by common thieves or, worst, by terrorist organizations. The biggest danger associated with unprotected RTG is their availability to terrorist groups, that can use radioactive material to manufacture the so-called "dirty bombs".

2. Methods

2.1 Source terms and accident scenarios

Case 1 – Cesium-137 release

It has been assumed that the amount of Cs-137 activity involved in the accident scenario is $1.11x10^{14}$ Bq. This amount of cesium is chosen for modeling because it is comparable to the amounts typically available in commercial radioactive sources.
The release scenario considers the introduction of the radionuclide inside a limestone fragmentation line and subsequent transmission to the filtration system, as shown in Figure 1.
The production plant considered in this case study is composed of three stacks and their characteristics are summarized in Table 1.

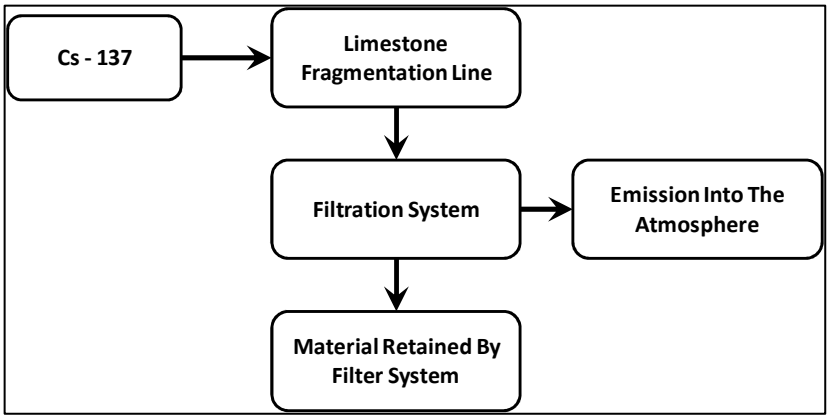

Fig. 1: Introduction of Radionuclide Inside the Cement Production Line

Table 1: Technical characteristics of stacks of cement production plant.

PROPERTY	STACK 1	STACK 2	STACK 3
Height above Sea Level	180 m	180 m	180 m
Physical stack height	92 m	92 m	92 m
Stack Diameter	3.1 m	1.8 m	1.8 m
Air Temperature	22°C	22°C	22°C
Stack Effluent Temperature	80°C	95°C	110°C
Stack Exit Velocity	17.5 m/s	10.4 m/s	8.2 m/s
Flue Gas Flow	475000 Nm^3/h	95000 Nm^3/h	75000 Nm^3/h

The raw material preparation stage of cement manufacture results in the production of a raw mix that is in a suitable state for feeding to the kiln in which it is converted by heat into clinker. From data obtained from the literature, it was possible to estimate the average hourly volume of raw material

sent to the oven, needed for the production of cement. In this work it has been assumed that during a typical production day, the raw materials sent to the production facilities are about 208 t/h, corresponding to $208x10^3$ kg/h, which is equivalent to $4.99x10^6$ kg/day. In this scenario, assuming that the filtration system works properly, the percentage of dust emitted into the atmosphere respect to the volume introduced into the system, is about 0.0033%.

In this case study, the source of Cs-137 was introduced through limestone fragmentation line, and radionuclide will be subject to the same filtration process of raw materials with emissions in atmosphere of 0.0033% of the initial amount. This estimation is conservative because we have assumed that Cs-137 is not all trapped in the clinker matrix. All the remaining radiogenic material will be retained by filters and/or reintroduced to cycle until its presence can be observed in the final product (clinker – cement). In order to analyze the release scenario a "virtual stack" has been defined, obtained by normalizing the characteristic parameters of each stack respect to the total flow rate, according to the following calculation scheme:

$$Q_T = Q_1 + Q_2 + Q_3 = 645.000\ Nm^3/h \quad (1)$$

$$d = d_1 \frac{Q_1}{Q_T} + d_2 \frac{Q_2}{Q_T} + d_3 \frac{Q_3}{Q_T} = 2,8\ m \quad (2)$$

$$v = v_1 \frac{Q_1}{Q_T} + v_2 \frac{Q_2}{Q_T} + v_3 \frac{Q_3}{Q_T} = 15,4\ m/s \quad (3)$$

$$T = T_1 \frac{Q_1}{Q_T} + T_2 \frac{Q_2}{Q_T} + T_3 \frac{Q_3}{Q_T} = 86°C \quad (4)$$

Where:

Q_T = Total gas flow rate.
Q_1, Q_2, Q_3 = Gas flow rate of single stack.
d = Stack diameter of virtual stack.
d_1, d_2, d_3 = Stack diameter of single stack.
v = Exit velocity of virtual stack.
v_1, v_2, v_3 = Exit velocity of single stack.
T = Effluent temperature of virtual stack.
T_1,T_2,T_3 = Effluent temperature of single stack.
Table 2: summarize the characteristic parameters of "virtual stack".

Table 2: Parameters of "virtual stack"

Height above sea level	180 m
Physical stack height	92 m
Stack diameter	2.8 m
Air temperature	22°C
Stack effluent temperature	86°C
Stack exit velocity	15.4 m/s
Flue gas flow	645.000 Nm^3/h

Case 2 – Strontium-90 release

The proposed scenario foresees a terrorist attack in the city of Rome, with the release of radioactive substances. The hypotheses is that a terrorist group acquires radioactive material from illegal market, consisting of 90Sr in the ceramic - glass form contained in the RTG type of a RTG IEU-1M (for further specifications see Table 3). This material allows to create a "dirty bomb" assembling Strontium to plastic explosive (readily available) and a remote trigger device. The bomb is secured inside the trunk of a car and the same is then placed in a short stop parking of Airport "Leonardo Da Vinci" of Rome, that is a rest area close to the airport and placed at a higher level than the road level (about 1.5 meters).

Table 3. Types and Main features of the RTG of Soviet manufacturing [38]

	RHS heat capacity, watts	RHS initial nominal activity, kilocuries	RTG electric capacity, watts	RTG mass, kilograms	Year of start of mass production
EFIR-MA	720	111	30	1250	1976
IEU-1	2200	49	80	2500	1976
IEU-2	580	89	14	600	1977
BETA - M	230	35	10	560	1978
GONG	315	49	18	600	1978
GOM	1100	170	60	1050 (3RHS – 90)	1983
IEU – 2M	690	106	20	600	1985
SENOSTAY	1870	288		1250	1989
IEU – 1M	2200 (3300)	340 (510)	120 (180)	2 (3) X 1050	1990

The choice of the Airport as place of the attack corresponds to the need to conduct realistic and meaningful assessments, considering a critical infrastructure provided by weather reports in constant and continuous updating, with a dedicated team of fire brigades. All the previous aspects make it possible to assess:

- the short term effects of the attack on "First responder" involved in emergency interventions and on people passing through the airport (with a diagram of Total Effective Dose Equivalent);
- the long-term effects resulting from the contamination of soil and groundwater (using the model "Ground deposition").

Once defined the total amount of the glass-ceramic matrix containing the radionuclide (42 Kg is the total quantity of the radionuclide contained in a commercial RTGs model IEU – 1M), the value of total activity of radioactive material was calculated , considering a decay time of 24 years (RTG's date of realization 1990, date of terrorist attack 2014) according to the formula:

$$A = A_0 e^{-\lambda t} \qquad (1)$$

We have assumed that the total activity of Sr-90 involved in the accident scenario is 7.0×10^{15} Bq.

Regarding the fraction of the radionuclide involved that is impacted in the release scenario, and the fraction of the radionuclide involved that passes through some confinement or filtration mechanism, these are assumed equal to one in case of explosion , according to the consideration of conservative nature that the entire quantity of the radioactive material is involved.

With regard to the fraction of the radionuclide involved that is aerosolized and released to the atmosphere, still following a conservative approach, it was assumed, on the basis of the findings from the study of KG Andersson [35], to consider a percentage of aerosolized material equal to 40% of the total. The parameter, called Respirable Fraction, is calculated as a percentage of the amount of aerosolized material of appropriate size to be assumed for inhalation (5-10 microns). Two hypotheses have been made on the basis of the results obtained by Pinnick [39] of a predicted percentage of breathable material equal to 10% and 20% of the total fraction of the aerosolized. Regarding the amount of explosive High explosive (TNT equivalent) were made two hypotheses (1lb , 3lb TNT) , to verify the influence of the effects of the explosion on the spread of the contaminant .

Table 4: Pasquill – Gifford stability classes and ground wind speed.[1]

Ground wind speed (m/s)	Sun high in sky	Sun low in sky or cloudy	Night time
1	A	B	F
2.5	A	C	E
3.5	B	C	D
5	C	D	D
7.5	C	D	D

2.2. Meteorological conditions and atmospheric stability classes used in HotSpot

Meteorologists distinguish several states of the local atmosphere: A, B, C, D, E, F. These states can be tabulated as a function of weather conditions, wind speed and time of day. According to the stability category the attack can result in a wide spectrum of lethal effects. Therefore the potential terrorist will certainly take that into account, just as it happens by war-planners, so that the lethal effects are maximized. The stability of the atmosphere depends on the temperature difference between an air parcel and the air surrounding it. Therefore, different levels of stability can occur based on how large or small the temperature difference is between the air Parcel and the surrounding air.[20-24, 31-34]

The stability classes used for this work are referred to Pasquill – Gifford stability classes and are depicted in Table 3. As can be seen in the Table, stabilities A, B, and C refer to daytime hours with unstable conditions. Stability D is representative of overcast days or nights with neutral conditions. Stabilities E and F refer to night-time, stable conditions and are based on the amount of cloud cover. Thus, classification A represents conditions of the greatest instability, and classification F reflects conditions of the greatest stability. For all stability class the wind direction was set at 270 degrees respect north direction. The values of wind speed assumed for the simulation are summarize in Table 4.

2.3. Radiation dose calculations

The calculations have been performed using HotSpot Version 2.07.1 and 3.0.1, running on a PC computer [25-28]. The "standard area terrain" type has been used to take into account the conservative condition because in this case the characteristic of roughness lengths is in the range of 0.01 – 0.1 meters. The deposition velocity of the particles is assumed to be 20 cm/s, whereas a value of 40 cm/s is used for the inhalable fraction.
The breathing rate of exposed person is based on the standard rates established by HotSpot code and taken from the International Commission on Radiological Protection (ICRP) [36]. The standard rate of 3.33 x 10^{-4} m^3/sec, equivalent to 1.2 m^3/hr has been considered: this value corresponding to light activity is recommended for doses received as a result of an accident. The height of the receptors is set to be 1.5 m. a typical value for breathing zone near the ground service.
Source term values used to establish the outline dose of TEDE and Ground Surface Deposition contour plot are shown in Table 5 (case 1) and Table 6 (case 2).

Table 5: Source term valued in HotSpot simulation

	TEDE (Sv)	GROUND SURFACE DEPOSITION (kBq/m^2)
Inner Contour Dose	$1.00x10^{-6}$	1
Middle Contour Dose	$1.00x10^{-7}$	0.1
Outer Contour Dose	$1.00x10^{-8}$	0.01

In the "second case set up" the threshold values relating to the Ground Deposition were kept as by default (Hotspot version 3.0.1), vice versa have been set new threshold values for the TEDE, to take account both of the risk associated with the exposure of the population, both to that of the first responder. The thresholds chosen were the following: inner contour dose (5 Sv) threshold for immediate deterministic effects; middle contour dose (0.02 Sv) max dose for first responders; outer contour dose (0.001 Sv) operational level for evacuation (Table 6). [36]

Table 6: Source term valued in HotSpot simulation

	TEDE (Sv)	GROUND SURFACE DEPOSITION (kBq/m^2)
Inner Contour Dose	5.00	3.700
Middle Contour Dose	$2.00x10^{-2}$	370
Outer Contour Dose	$1.00x10^{-3}$	37

To evaluate the dose conversion factors in HOTSPOT, we referred to the publication FGR 11 when we used the software version 2.07.1, to the publication FGR 13 with version 3.0.1. For the purpose of this work, the sample time has been set to 60 minutes for "the Cs-137 case" and 10 minutes for "the Sr-90 case"; in both cases the holdup time is assumed 0 minutes, to simulate that the material is immediately released into the atmosphere.
All simulation scenarios have been performed including plume passage inhalation and submersion, ground shine (without the weathering correction factor) and re-suspension (with re-suspension factor obtained from [4]).

3. Results

It was carried out a sensitivity analysis of the values of TEDE and Ground Deposition in function of 3 parameters:
• Weather stability classes (1°and 2°case study).
• Respirable Fraction (2° case study).
• Pounds of Explosive used (2°case study).
The first case study was useful to test for realistic and reliable estimation of contamination (total dose, ground deposition etc.), following a typical dispersion of radiological materials into the atmosphere not connected to an explosion event. The second case study was thought to qualitatively verify the dependence of TEDE and Ground Deposition as a functions of explosive release typical parameters (explosive amount, respirable fraction released).

<u>Cs-137 case study – dependence on weather stability classes</u>
In order to define all boundary conditions it is necessary to know the cloud properties:
- dimensions (volume, effective height);
- particles size distribution within the cloud;

and all the functions of the source term amount, space and time, wind speed and atmospheric stability class.

In this section the graphic results obtained for any scenario considered are reported.

For each class of stability and wind speed value the diagrams TEDE and Ground Deposition diagrams have been plotted as function of downwind distance.

The doses calculated could be received by a person at height of 1.5 m from ground level who remained within the plume for the entire duration of the cloud passage. As the release occurs at 92 m stack height, the doses first increase with distance, reach a maximum value and then decrease.

The heat and smoke will lift small particles of Cesium up into the air and, according to the nature of the released radioactive material, these particles will settle to the ground as they are carried along by the wind contaminating the ground surface. Large particles will contaminate the immediate vicinity of the stack while smaller (fine and mostly inhalable) ones will travel large distances or will rise up at high altitudes until they are deposited on the ground. Obviously, non-inhalable material will have a much larger deposition velocity than inhalable ones.

Table 2 summarizes some physical parameters obtained from the Hotspot simulations.

Setting the wind speed and the geometry of the stack, the change of atmospheric stability class affects the distance at which the maximum dose occurs, the TEDE variation and the effective height of release.

In Figure 2 the diagram of the Total Effective Dose Equivalent as a function of downwind distance is shown. The location of the maximum dose gives the plume touchdown distance. For all Scenario considered, it can be observed that the plume touchdown distance (point of maximum dose) increases with increasing of the stability, however the maximum dose value reduces with increasing of the stability. Only for Scenario 1, for the Pasquill stability class F, the inner dose did not exceed. On the other hand, the worst case represented by the case Scenario 2 for the stability class A.

Table 7: Main parameters obtained for HotSpot code

SCENARIO 1			
	Stability Class A	**Stability Class B**	**Stability Class F**
Effective Release Height	432 m	432 m	149 m
Maximum Dose Distance	1.4 km	2.2 Km	23 Km
Maximum TEDE	6.25×10^{-6} Sv	4.16×10^{-6} Sv	1.08×10^{-7} Sv
Exceeds inner dose out to	4.5 Km	5.5 Km	Not Exceeded
Exceeds middle dose out to:	12.5 Km	13.6 Km	30 Km
Exceeds outer dose out to	34.6 Km	32.9 Km	74 Km
SCENARIO 2			
	Stability Class A	**Stability Class C**	**Stability Class E**
Effective Release Height	234 m	222 m	152 m
Maximum Dose Distance	0.82 km	2.2 Km	8.1 Km
Maximum TEDE	1.18×10^{-5} Sv	$7 \times .81 \times 10^{-6}$ Sv	1.39×10^{-6} Sv
Exceeds inner dose out to	4.12 Km	8.9 Km	12.5 Km
Exceeds middle dose out to:	13.05 Km	23.2Km	36 Km
Exceeds outer dose out to	43.51 Km	51 Km	58.10 Km
SCENARIO 3			
	Stability Class B	**Stability Class C**	**Stability Class D**
Effective Release Height	195 m	186 m	174 m
Maximum Dose Distance	1.1 Km	1.8 Km	4.4 Km
Maximum TEDE	1.05×10^{-5} Sv	8.52×10^{-6} Sv	3.11×10^{-6} Sv
Exceeds inner dose out to	5.3 Km	8.6 Km	12.9 Km
Exceeds middle dose out to:	16.7 Km	25.9 Km	30.7 Km
Exceeds outer dose out to	55.8 Km	64.1 Km	49 Km
SCENARIO 4			
	Stability Class C		**Stability Class D**
Effective Release Height	159 m		151 m
Maximum Dose Distance	1.5 Km		3.5 Km
Maximum TEDE	8.54×10^{-6} Sv		3.5×10^{-6} Sv

Exceeds inner dose out to	7.8 Km	12.4 Km
Exceeds middle dose out to:	26.7 Km	32.6 Km
Exceeds outer dose out to	78.3 Km	58.6 Km
SCENARIO 5		
	Stability Class C	**Stability Class D**
Effective Release Height	137 m	132 m
Maximum Dose Distance	1.3 Km	3 Km
Maximum TEDE	$8.07x10^{-6}$Sv	$3.65x10^{-6}$Sv
Exceeds inner dose out to	6.8 Km	11.7 Km
Exceeds middle dose out to	26.5 Km	35 Km
Exceeds outer dose out to	93.6 Km	73.7 Km

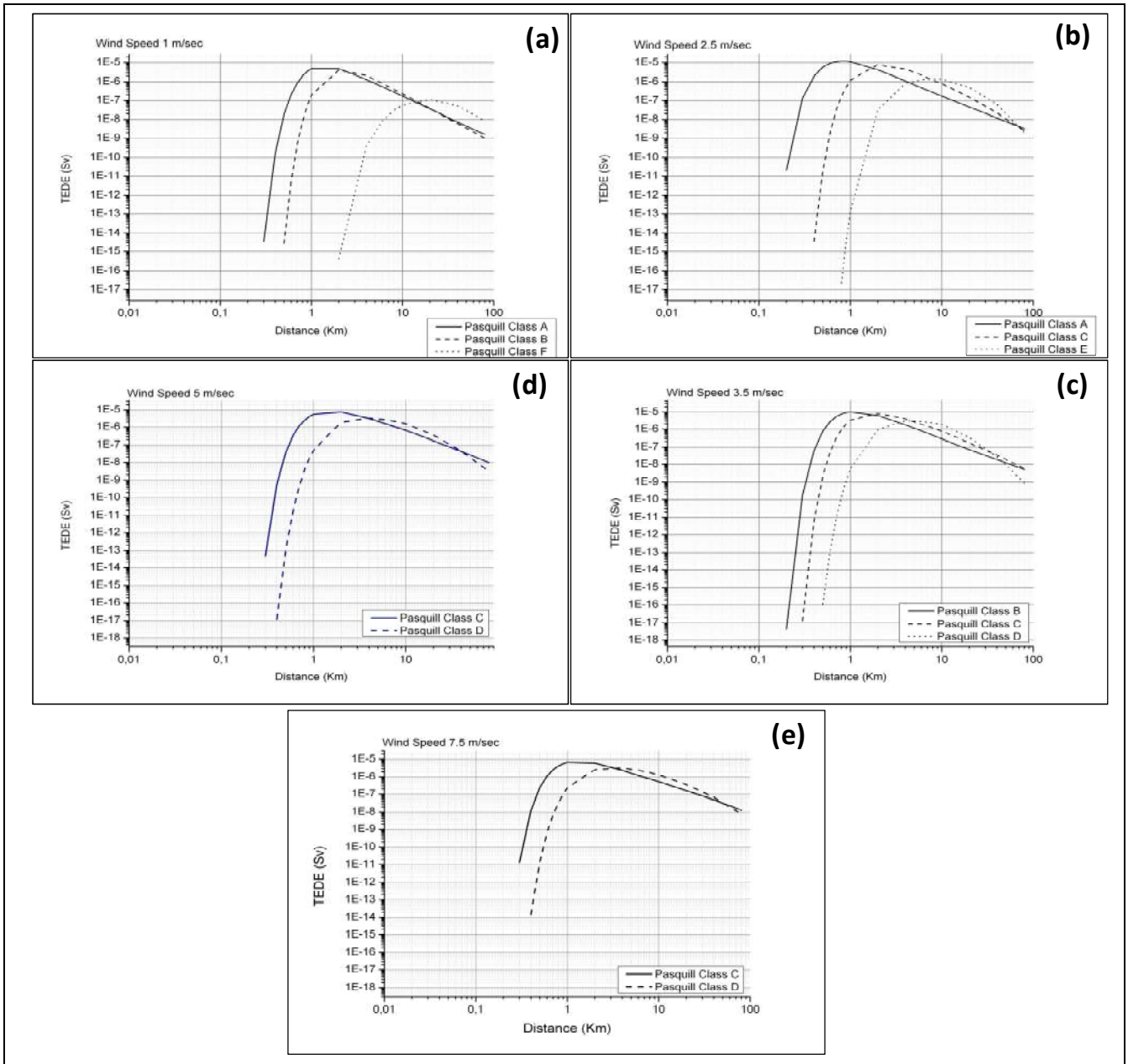

Fig. 2: Total Effective Dose Equivalents vs downwind distance: (a): Scenario 1; (b) Scenario 2; (c) Scenario 3; (d) Scenario 4; (e) Scenario 5

Atmospheric processes can reduce or enhance dispersion and deposition after the initial release of radiological source. Three of the most important parameters that drive the phenomena are wind speed, atmospheric stability, and precipitation. Dilution occurs most rapidly at high wind speeds, with unstable atmospheric condition with sharp temperature gradients in which the surface layer is hotter than the air above it, and during precipitation. For these reasons, in this case study The Ground Surface Deposition as function of downwind distance has been evaluated. The Figure 3 shown the diagram for each Scenario considered.

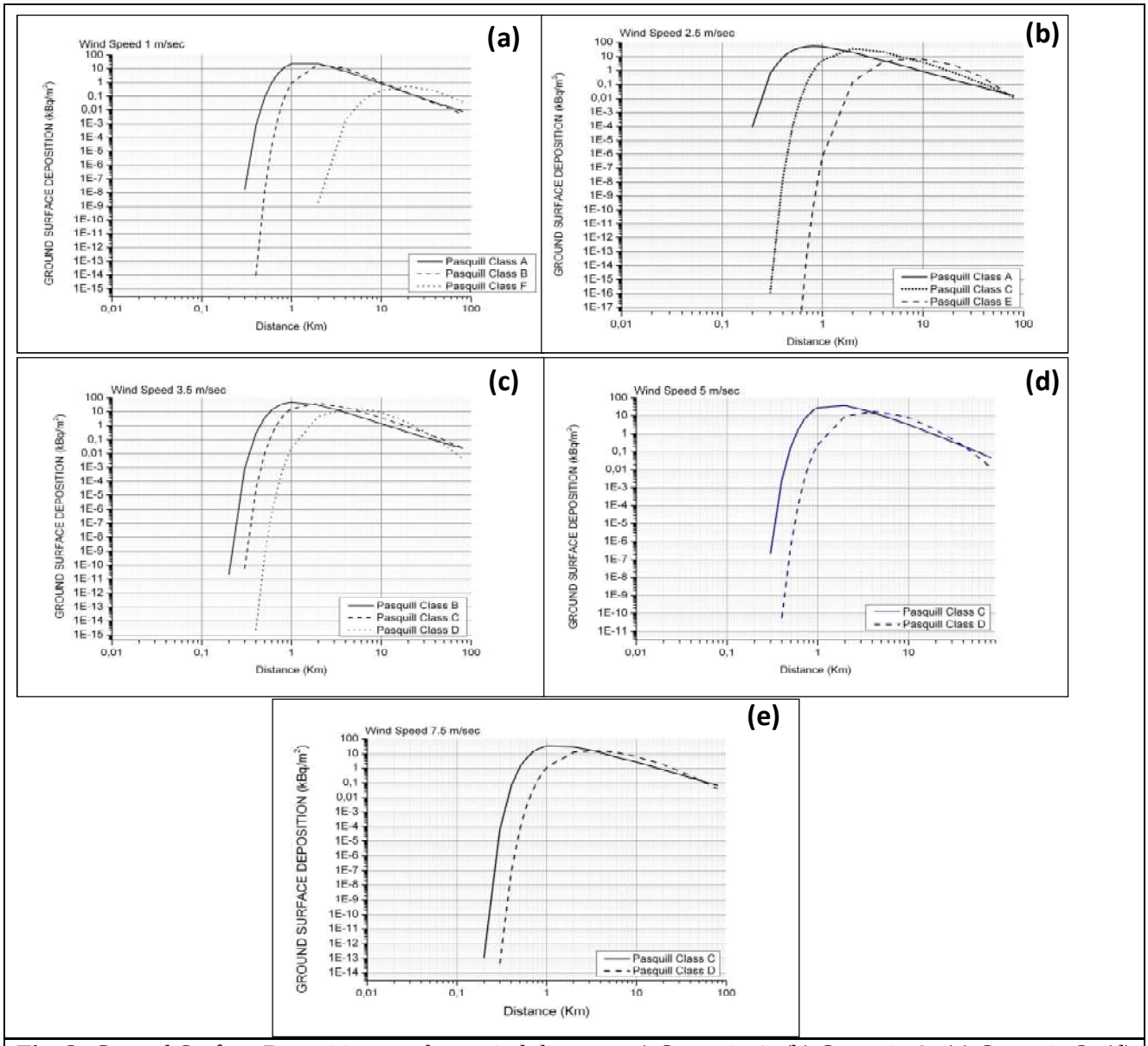

Fig. 3: Ground Surface Deposition vs. downwind distance: a) Scenario 1; (b) Scenario 2; (c) Scenario 3; (d) Scenario 4; (e) Scenario 5.

There are several relationships between ground-level concentrations and concentrations at the level of the plume release point in function of meteorological conditions.

For example in plume characterized by high concentration of dispersed material, pollutants may reach the ground level after a short distance in case of fumigation conditions (clean skies and light winds); when the lapse rate changes from unstable to stable in stack proximity. With small different height (ΔH), the fumigation can occur close to the source but will be of relatively short duration. For large ΔH, the fumigation will occur some distance from the stack (perhaps 30 to 40 km), but can persist for a longer time interval. Concentrations considerably lower than those associated to

fumigation, but of significance, can occur with neutral or unstable conditions when the dispersion upward is severely limited by the existence of a more stable layer above the plume, for example, an inversion. Under stable conditions the maximum concentration at ground-level from big amount of material are less than those occurring under unstable conditions and occur at greater distances from the source. Because the maximum occurs at greater distances, concentrations that are below the maximum but still significant can occur over large areas. This becomes increasingly significant if the emissions are from more than one source.
Figure 4 summarizes the trends of curves for each stability class considered.

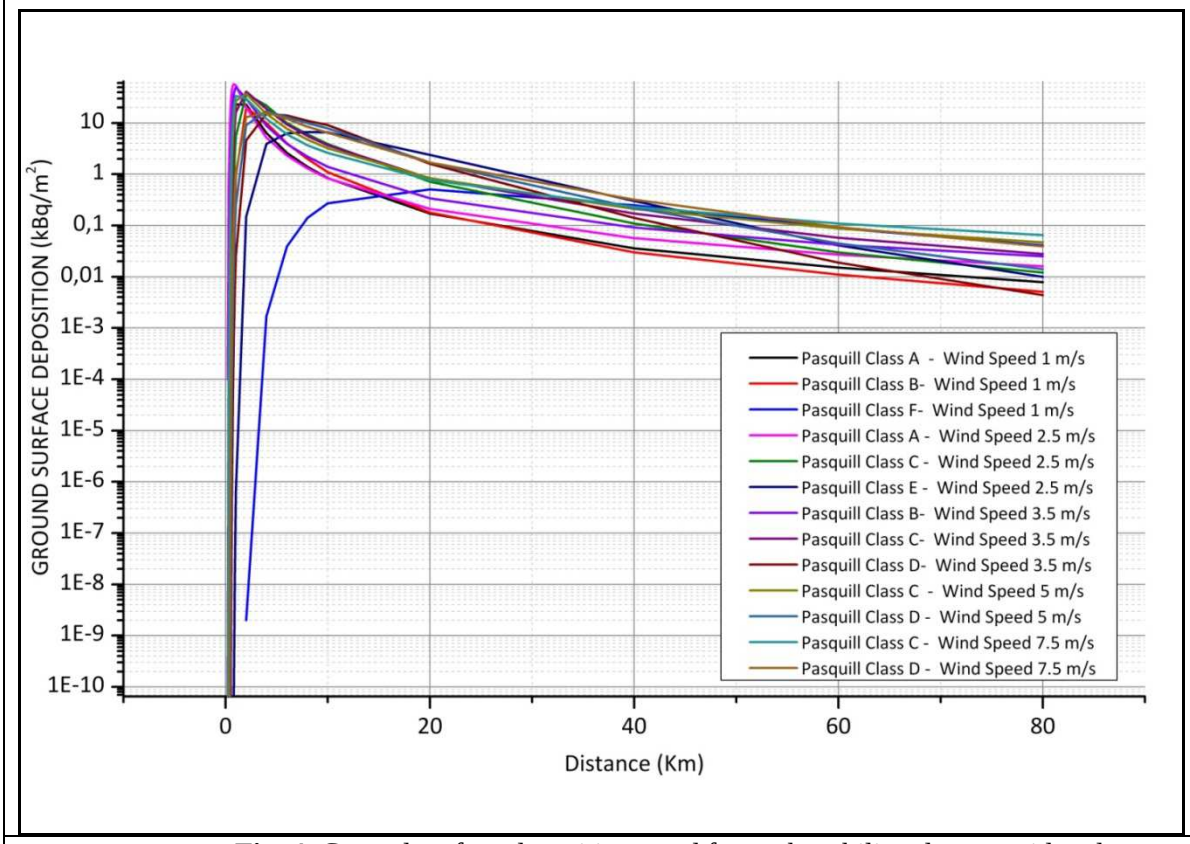

Fig. 4: Ground surface deposition trend for each stability class considered.

<u>Sr-90 case study – dependence on respirable fraction, pounds of explosive used, weather stability classes</u>
In this case was carried out a sensitivity analysis of the values of TEDE and Ground Deposition in function of n° 3 parameters:
• Respirable Fraction: 20% - 40% of the aerosolized fraction.
• Explosive Pounds used: 1lb (0,45Kg) – 3lb (1,36Kg) TNT equivalent.
• Classes weather: moderatly unstable (Pasquill class B: "PasB") - neutral (Pasquill class D: "PasD").
In this way were generated n° 8 cases type:
Respirable Fraction = 20%:
1) 20C_1TNT_PasB
2) 20C_1TNT_PasD
3) 20C_3TNT_PasB
4) 20C_3TNT_PasD
Respirable Fraction = 10%:
5) 10C_1TNT_PasB
6) 10C_1TNT_PasD
7) 10C_3TNT_PasB
8) 10C_3TNT_PasD
Several HotSpot simulations allowed the comparison between the cases. The dependence of the TEDE and Ground Deposition compared to the change of weather stability classes was made possible thanks to the specific software function "All stability classes graph" which allows to generate a Total Effective Dose Graph Ground Deposition and a graph containing the trends relating to all classes of stability. The general trend confirm that dispersions affecting larger areas are

associated to increasing stability classes. Further observations were conducted comparing the output produced by the software (TEDE and Ground Deposition), in terms of:

•Areas (Km^2) affected by contamination.

•Maximum size of the area affected by contamination (Km).

•Maximum height reached by the material involved in the explosion (m).

Referring to TEDE Table 8 summarizes parameters obtained from the Hotspot simulations for each case study.

Table 8: Comparison of Total Effective Dose Equivalents values between the 8 case study

	TEDE			
MIDDLE CONTOUR DOSE(0,02Sv)	**Respirable Fraction 20%**		**TNT equiv. =1lb**	**TNT equiv. =3lb**
			20C_1TNT_PasB	*20C_3TNT_PasB*
	Pasquill class B	Middle dose Area	0,053 Km^2	0,05 Km^2
		Max length middle cont.	0,032 Km	0,032 Km
		Max Plume Height	76 m	100 m
			20C_1TNT_PasD	*20C_3TNT_PasD*
	Pasquill class D	Middle dose Area	0,09 Km^2	0,076 Km^2
		Max length middle cont.	0,6 Km	0,6 Km
		Max Plume Height	76 m	100 m
	Respirable Fraction 10%			
			10C_1TNT_PasB	*10C_3TNT_PasB*
	Pasquill class B	Middle dose Area	0,028 Km^2	0,026 Km^2
		Max length middle cont.	0,25 Km	0,21 Km
		Max Plume Height	76 m	100 m
			10C_1TNT_PasD	*10C_3TNT_PasD*
	Pasquill class D	Middle dose Area	0,04 Km^2	0,033 Km^2
		Max length middle cont.	0,4 Km	0,3 Km
		Max Plume Height	76 m	100 m
OUTER CONTOUR DOSE(0,001Sv)	**Respirable Fraction 20%**		**TNT equiv. =1lb**	**TNT equiv. =3lb**
			20C_1TNT_PasB	*20C_3TNT_PasB*
	Pasquill class B	Outer dose Area	0,87 Km^2	0,83 Km^2
		Max length outer cont.	1,56 Km	1,5 Km
		Max Plume Height	76 m	100 m
			20C_1TNT_PasD	*20C_3TNT_PasD*
	Pasquill class D	Outer dose Area	3,1 Km^2	2,8 Km^2
		Max length outer cont.	5 Km	4,7 Km
		Max Plume Height	76 m	100 m
	Respirable Fraction 10%			
			10C_1TNT_PasB	*10C_3TNT_PasB*
	Pasquill class B	Outer dose Area	0,46 Km^2	0,44 Km^2
		Max length outer cont.	1,1 Km	1,1 Km
		Max Plume Height	76 m	100 m
			10C_1TNT_PasD	*10C_3TNT_PasD*
	Pasquill class D	Outer dose Area	1,3 Km^2	1,2 Km^2
		Max length outer cont.	3,1 Km	2,8 Km
		Max Plume Height	76 m	100 m

It is evident that value over the 5Sv are never reached Taking into account the exposure limits for operators (0,02 Sv/yr) and for population (0,001 Sv/yr) we can assume that regarding the TEDE has been verified that, the increase of the respirable fraction (RF) (calculated on the total component of the material aerosolized by the explosion) increases the areas affected by the plume. Conversely, the increase of the explosives used determines an increase in the maximum height of the plume (from 76m to 100m). Referring to Ground deposition Table 9 summarizes parameters obtained from the software simulations

Table 9: Comparison of Ground deposition values between the 8 case study

GROUND DEPOSITION				
INNER CONTOUR (3.700KBq/mq)	**Respirable Fraction 20%**		**TNT equiv. =1lb**	**TNT equiv. =3lb**
			20C_1TNT_PasB	*20C_3TNT_PasB*
	Pasquill class B	Inner dose Area	16 Km^2	16 Km^2
		Max length inner cont.	7 Km	7 Km
		Max Plume Height	76 m	100 m
			20C_1TNT_PasD	*20C_3TNT_PasD*
	Pasquill class D	Inner dose Area	40 Km^2	45 Km^2
		Max length inner cont.	20 Km	23 Km
		Max Plume Height	76 m	100 m
	Respirable Fraction 10%		*10C_1TNT_PasB*	*10C_3TNT_PasB*
	Pasquill class B	Inner dose Area	17 Km^2	18 Km^2
		Max length inner cont.	8 Km	8,5 Km
		Max Plume Height	76 m	100 m
			10C_1TNT_PasD	*10C_3TNT_PasD*
	Pasquill class D	Inner dose Area	43 Km^2	50 Km^2
		Max length inner cont.	23 Km	25 Km
		Max Plume Height	76 m	100 m
MIDDLE CONTOUR (370KBq/mq)	**Respirable Fraction 20%**		**TNT equiv. =1lb**	**TNT equiv. =3lb**
			20C_1TNT_PasB	*20C_3TNT_PasB*
	Pasquill class B	Middle dose Area	96 Km^2	98 Km^2
		Max length middle cont.	24 Km	23 Km
		Max Plume Height	76 m	100 m
			20C_1TNT_PasD	*20C_3TNT_PasD*
	Pasquill class D	Middle dose Area	224 Km^2	261 Km^2
		Max length middle cont.	60 Km	64 Km
		Max Plume Height	76 m	100 m
	Respirable Fraction 10%		*10C_1TNT_PasB*	*10C_3TNT_PasB*
	Pasquill class B	Middle dose Area	104 Km^2	107 Km^2
		Max length middle cont.	29 Km	25 Km
		Max Plume Height	76 m	100 m
			10C_1TNT_PasD	*10C_3TNT_PasD*
	Pasquill class D	Middle dose Area	239 Km^2	279 Km^2
		Max length middle cont.	62,5 Km	70 Km
		Max Plume Height	76 m	100 m
OUTER CONTOUR (37KBq/mq)	**Respirable Fraction 20%**		**TNT equiv. =1lb**	**TNT equiv. =3lb**
			20C_1TNT_PasB	*20C_3TNT_PasB*
	Pasquill class B	Outer dose Area	556 Km^2	570 Km^2
		Max length outer cont.	72 Km	73 Km
		Max Plume Height	76 m	100 m
			20C_1TNT_PasD	*20C_3TNT_PasD*
	Pasquill class D	Outer dose Area	990 Km^2	1000 Km^2
		Max length outer cont.	151 Km	163 Km
		Max Plume Height	76 m	100 m
	Respirable Fraction 10%		*10C_1TNT_PasB*	*10C_3TNT_PasB*
	Pasquill class B	Outer dose Area	608 Km^2	622 Km^2
		Max length outer cont.	63 Km	76 Km
		Max Plume Height	76 m	100 m
			10C_1TNT_PasD	*10C_3TNT_PasD*
	Pasquill class D	Outer dose Area	1000 Km^2	1000 Km^2
		Max length outer cont.	150 Km	163 Km
		Max Plume Height	76 m	100 m

Regarding the values obtained from Ground Deposition model, all the thresholds set to delimit the contamination areas are exceeded.
In opposition to the trend determined for TEDE, with the increase of the respirable fraction (RF) of the total component of the material aerosolized decreases the surface of the areas affected by the plume. The increase in the amount of explosives used in addition to determining an increase in the maximum height of the plume (from 76m to 100m) also increases the size of the areas.

4. Conclusions

The authors have analyzed Different scenarios of radiological release in atmosphere, and the connected plume extension related to the ground surface deposition. The boundary condition used are referred to: type of radioactive material, stack geometry and dimension, effluent parameters and meteorological conditions, respirable fraction amount of the explosive involved.
The results indicate a relatively small amount of Cs-137 has the potential to contaminant a relatively large area with the extent of contamination dependent on Cs-137 particle size, the height of release, and local weather conditions. While at the end of the evaluation, resulting from the explosion of a dirty bomb (containing strontium-90), it can be observed that the values of TEDE obtained through the software show the absence of risk of immediate deterministic effects (5SV). However, the simulations show the presence of areas between 0.03 km^2 and 0.09 km^2 , with values of TEDE of (0.02 Sv), values so high to require the immediate evacuation of the area, and the shift of rescue teams. Modeling the dispersion of radioactive aerosols throughout an urban landscape, especially with accurate knowledge of radionuclide, geometry of source and meteorology, is essential for assessing the potential consequences of a terrorist incident and implementing effective emergency response, health services, and decontamination decisions.
Considering that the atmospheric release of radioactive material might occur at high-density crowd events or in densely – populated urban areas, it is possible to envisage that thousands of people might be exposed to ionizing radiation. Additionally, operations in these contaminated areas might result in intervention teams receiving sufficient radiation doses that are of particular concern and should be managed. [29,30,37]
For first responders, given the dominance of the inhalation pathway, the modeling results underscore the importance of adequate respiratory protection to reduce the amount of radioactive material inhaled. And, prior to initiating follow-up evacuation and environmental remediation activities, the results also emphasize the importance of initial screening to delineate quickly TEDE "boundary lines" as a beginning point for determining the extent of the "hot zone" for potential ground shine exposure created by accidental radiological release
This application of computer modeling has implications for identifying the potential consequences of an intentional or unintentional radiological releases. The consequence data obtained from this study can be used for the establishment of response measures against radiological terror.
The authors can assess that the HotSpot code is a useful tool to give a quick answer about the radiological contamination in the "hot zone". It is very important to optimize the rescue operations of first responders and to allow safe routes way to the population. In order to enhance the effectiveness of the HotSpot code it is necessary compare the simulation results with an higher quantity of in-field data. This task, together to the geo-referencing of numerical data, represent two of the main future development of this work.

References:

1. R.R. Draxler, Determination of amospheric diffusion parameters, *Atmospheric Environment*, Vol.10, No.2, 1976, pp. 99-105.
2. International Atomic Energy Agency, *The radiological Incident in Goiania*, Pub. 815, Vienna 1988.
3. Y. Rentai, Atmospheric dispersion of radioactive material in radiological risk assessment and emergency response, *Progress in Nuclear Science and Technology*, Vol 1, 2011, pp. 7-13.
4. Report No.129 of National Council on Radiation Protection and Measurements, 1999).
5. Gaudio, P., Malizia, A., Lupelli, I. "Experimental and numerical analysis of dust resuspension for supporting chemical and radiological risk assessment in a nuclear fusion device" (2010) International Conference on Mathematical Models for Engineering Science - Proceedings, pp. 134-147
6. P Gaudio, Malizia A., I Lupelli (2011). RNG k-e modelling and mobilization experiments of loss of vacuum in small tanks for nuclear fusion safety applications. "International journal of systems applications, engineering & development", vol. 5; p. 287-305, ISSN: 2074-1308
7. Benedetti, M., Gaudio, P., Lupelli, I., Malizia, A., Porfiri, M.T., Richetta, M. "Large eddy simulation of Loss of Vacuum Accident in STARDUST facility" (2013) Fusion Engineering and Design, . Article in Press.
8. M.Benedetti, P.Gaudio, I.Lupelli, Malizia A., M.T.Porfiri, M.Richetta (2011). Influence of Temperature Fluctuations, Measured by Numerical Simulations, on Dust Resuspension Due to L.O.V.As . International journal of systems applications, engineering & development, vol. 5; p. 718-727, ISSN: 2074-1308
9. Bellecci, C., Gaudio, P., Lupelli, I., Malizia, A., Porfiri, M.T., Quaranta, R., Richetta, M. "Validation of a loss of vacuum accident (LOVA) Computational Fluid Dynamics (CFD) model" (2011) Fusion Engineering and Design, 86 (9-11), pp. 2774-2778.
10. Bellecci, C., Gaudio, P., Lupelli, I., Malizia, A., Porfiri, M.T., Quaranta, R., Richetta, M. "STARDUST experimental campaign and numerical simulations: Influence of obstacles and temperature on dust resuspension in a vacuum vessel under LOVA" (2011) Nuclear Fusion, 51 (5), art. no. 053017
11. Bellecci, C., Gaudio, P., Lupelli, I., Malizia, A., Porfiri, M.T., Quaranta, R., Richetta, M. "Loss of vacuum accident (LOVA): Comparison of computational fluid dynamics (CFD) flow velocities against experimental data for the model validation" (2011) Fusion Engineering and Design, 86 (4-5), pp. 330-340.
12. Benedetti, M., Gaudio, P., Lupelli, I., Malizia, A., Porfiri, M.T., Richetta, M. "Scaled experiment for Loss of Vacuum Accidents in nuclear fusion devices: Experimental methodology for fluid-dynamics analysis in STARDUST facility" (2011) Recent Researches in Mechanics - Proc. of the 2nd Int. Conf. on FLUIDSHEAT'11, TAM'11,Proc. of the 4th WSEAS Int. Conf. UPT'11, CUHT'11, pp. 142-147.
13. Pinna, T., Cadwallader, L.C., Cambi, G., Ciattaglia, S., Knipe, S., Leuterer, F., Malizia, A., Petersen, P., Porfiri, M.T., Sagot, F., Scales, S., Stober, J., Vallet, J.C., Yamanishi, T. "Operating experiences from existing fusion facilities in view of ITER safety and reliability" (2010) Fusion Engineering and Design, 85 (7-9), pp. 1410-1415
14. C Bellecci, P Gaudio, I Lupelli, Malizia A., M T Porfiri, R Quaranta, M Richetta (2010). Validation of a Loss Of Vacuum Accident (LOVA) computational fluid dynamics (cfd) model. In: Proceedings 26th Symposium on Fusion Technology. Porto, Portugal, 27 September-1 October 2010
15. Bellecci, C., Gaudio, P., Lupelli, I., Malizia, A., Porfiri, M.T., Quaranta, R., Richetta, M."Experimental mapping of velocity flow field in case of L.O.V.A inside stardust facility" (2010) 37th EPS Conference on Plasma Physics 2010, EPS 2010, 2, pp. 703-706.
16. P.Gaudio, Malizia A., I. Lupelli (2010). Experimental and Numerical Analysis of Dust Resuspension for Supporting Chemical

and Radiological Risk Assessment in a Nuclear Fusion Device. In: Conference Proceedings - International Conference on Mathematical Models for Engineering Science (MMES' 10). Puerto De La Cruz, Tenerife, 30/11/2010 - 30/12/2010, p. 134-147, ISBN/ISSN: 978-960-474-252-3

17. Bellecci, C., Gaudio, P., Lupelli, I., Malizia, A., Porfiri, M.T., Quaranta, R., Richetta, M. "Characterization of divertor influence in case of LOVA: CFD analysis of stardust experimental facility" (2009) 36th EPS Conference on Plasma Physics 2009, EPS 2009 - Europhysics Conference Abstracts, 33 E1, pp. 266-269.
18. C.Bellecci, P.Gaudio, I. Lupelli, Malizia A., M.T.Porfiri, R.Quaranta, M. Richetta (2009). Velocity flow field characterization inside STARDUST experimental facility: Comparison between experimental campaign and numerical simulation results. In: ICENES2009 Proceedings. Ericeria-Portugal, 29 June- 3 July 2009, ISBN/ISSN: 978-989-96542-1-1
19. C. Bellecci, P. Gaudio, I. Lupelli, Malizia A., M.T.Porfiri, M. Richetta (2008). Dust mobilization and transport measures in the STARDUST facility. In: EPS2008 Proceedings, 35th EPS Conference on Plasma Physics. Hersonissos - Crete - Greece, 9 - 13 June 2008, vol. ECA Vol.32, p. P-1.175
20. P. Gaudio, M. Gelfusa, I. Lupelli, Malizia A., A. Moretti, M. Richetta, C. Serafini (2012). Early forest fires detection using a portable CO2 Dial system: preliminary results. In: Proceedings 14° Convegno Nazionale delle Tecnologie Fotoniche, Firenze, 15-17 maggio 2012 – ISBN . Firenze, Italia, Maggio 2012, ISBN/ISSN: 9788887237146.
21. P.Gaudio, M. Gelfusa, Malizia A., M. Richetta, C.Serafini, P. Ventura, C. Bellecci, L.De Leo, T.Lo Feudo, A. Murari (2012). A portable LIDAR system for the early detection: FfED system - a case study. In: Advances in Fluid Mechanics and Heat & Mass Transfer Conference Proceedings. Istanbul - Turkey, July 21-23, 2012, p. 208-214, ISBN/ISSN: 978-1-61804-114-2
22. Gaudio, P., Gelfusa, M., Lupelli, I., Malizia, A., Moretti, A., Richetta, M., Serafini, C., Bellecci, C."First open field measurements with a portable CO2 lidar/ dial system for early forest fires detection" (2011) Proceedings of SPIE - The International Society for Optical Engineering, 8182, art. no. 818213
23. Bellecci, C., Gaudio, P., Gelfusa, M., Malizia, A., Richetta, M., Serafini, C., Ventura, P. "Planetary Boundary Layer (PBL) monitoring by means of two laser radar systems: Experimental results and comparison" (2010) Proceedings of SPIE - The International Society for Optical Engineering, 7832, art. no. 78320X.
24. [24] Bellecci, C., Gaudio, P., Gelfusa, M., Lo Feudo, T., Malizia, A., Richetta, M., Ventura, P. "Raman water vapour concentration measurements for reduction of false alarms in forest fire detection"
(2009) Proceedings of SPIE - The International Society for Optical Engineering, 7479, art. no. 74790H
25. Gallo, R., De Angelis, P., Malizia, A., Conetta, F., Di Giovanni, D., Antonelli, L., Gallo, N., Fiduccia, A., D'Amico, F., Fiorito, R., Richetta, M., Bellecci, C., Gaudio, P. "Development of a georeferencing software for radiological diffusion in order to improve the safety and security of first responders" (2013) Defence S and T Technical Bulletin, 6 (1), pp. 21-32.
26. Malizia, A., Quaranta, R., Mugavero, R., Carcano, R., Franceschi, G."Proposal of the prototype RoSyD-CBRN, a robotic system for remote detection of CBRN agents" (2011) Defence S and T Technical Bulletin, 4 (1), pp. 64-76
27. Malizia, A., Lupelli, I., D'Amico, F., Sassolini, A., Fiduccia, A., Quarta, A.M., Fiorito, R., Gucciardino, A., Richetta, M., Bellecci, C., Gaudio, P."Comparison of software for rescue operation planning during an accident in a nuclear power plant" (2012) Defence S and T Technical Bulletin, 5 (1), pp. 36-45.

28. R Gallo, P De Angelis, N Gallo, Malizia A., A Fiduccia, F D'Amico, R Fiorito, A Gucciardino, M Richetta, C Bellcci, P Gaudio (2012). Development of a software for the identification mapping of radiological diffusion in order to improve the rescue operations. In: MIMOS Conference Proceedings. Roma, 9-11 Ottobre 2012
29. Malizia A., R.Quaranta, R.Mugavero, R.Carcano, G.Franceschi (2011). Proposal of the prototype RoSyD-CBRN, a robotic system for remote detection of CBRN agents. Defence S&T technical bulletin, vol. 4; p. 64-76, ISSN: 1985-6571
30. Cenciarelli, O., Malizia, A., Marinelli, M., Pietropaoli, S., Gallo, R., D'Amico, F., Bellecci, C., Fiorito, R., Gucciardino, A., Richetta, M., Gaudio, P. "Evaluation of biohazard management of the Italian national fire brigade "(2013) Defence S and T Technical Bulletin, 6 (1), pp. 33-41.
31. Bellecci, C., De Leo, L., Gaudio, P., Gelfusa, M., Lo Feudo, T., Martellucci, S., Richetta, M. "Reduction of false alarms in forest fire surveillance using water vapour concentration measurements (2009) Optics and Laser Technology, 41 (4), pp. 374-379.
32. Bellecci, C., De Leo, L., Gaudio, P., Gelfusa, M., Lo Feudo, T., Martellucci, S., Richetta, M."Evolution study of smoke backscattering coefficients in a cell by means of a compact mobile Nd:YAGlidar system" (2008) Proceedings of SPIE - The International Society for Optical Engineering, 6745, art. no. 67451S, .
33. Bellecci, C., Francucci, M., Gaudio, P., Gelfusa, M., Martellucci, S., Richetta, M., Lo Feudo, T. "Application of a CO2 dial system for infrared detection of forest fire and reduction of false alarm" (2007) Applied Physics B: Lasers and Optics, 87 (2), pp. 373-378.
34. Bellecci, C., De Leo, L., Gaudio, P., Gelfusa, M., Lo Feudo, T., Martellucci, S., Richetta, M."Water vapour emission in vegetable fuel: Absorption cell measurements and detection limits of our CO2 Dial system " (2006) Proceedings of SPIE - The International Society for Optical Engineering, 6367, art. no. 63670I, .
35. K.G. Andersson , T. Mikkelsen , P. Astrup , S. Thykier-Nielsen , L.H. Jacobsen , L.Schou-Jensen , S.C. Hoe & S.P. Nielsen. "Estimation of health hazards resulting from a radiological terrorist attack in a city" - Radiat Prot Dosimetry. 2008;131:297–307.
36. International Commission on Radiological Protection; 1990 Recommendations of the International Commission on Radiological Protection; ICRP 60; ICRP Vol. 21/1-3; ISBN-13: 978-0-08-041144-6; Elsevier Publication (1991)
37. Malizia A., Quaranta R., Mugavero R.,"CBRN events in the subway system of Rome: Technical-managerial solutions for risk reduction", 2010, Defence S and T Technical Bulletin". vol. 33; p. 140-157, ISSN: 1985-6571
38. Information partly taken from: A.M.Agapov, G.A. Novikov, Radiologichesky terrorism. http://www.informatom.ru/rus/safe/vena/Vena.asp (In Russian), and M.I.Rylov, M.N.Tikhonov. Problemy radiatsionnoi bezopasnosti.//Atomnaya strategiya, St. Petersburg, N1(6) June 200, p. 32. (In Russian).
39. Pinnick, R.G., Fernandez, G. & Hinds, B.D. (1983). Explosion dust particle size measurements, Applied Optics 22 (1), pp. 95-102.
40. NIST Nuclide Half-Life Measurements, NIST, Retrieved 13 March 2011. http://www.nist.gov/pml/data/halflife.cfm
41. Orphan Sources US Nuclear Regulatory Commission, Nuclear materials. http://www.nrc.gov/materials/miau/miau-reg-initiatives/orphan.htm